Hindawi
Advances in Polymer Technology
Volume 2020, Article ID 6582825, 13 pages
https://doi.org/10.1155/2020/6582825

Research Article

Nuclear-Targeting Delivery of CRISPRa System for Upregulation of β-Defensin against Virus Infection by Dexamethasone and Phenylalanine Dual-Modified Dendrimer

Mingxiang Zuo,[1] **Xiaoxia Li**,[1] **Shuang Liu**,[2] **Bin Chen**,[3] **and Du Cheng**[1]

[1]*PCFM Lab of Ministry of Education, School of Materials Science and Engineering, Sun Yat-sen University, Guangzhou 510275, China*
[2]*Zhongshan School of Medicine, Sun Yat-sen University, Guangzhou 510275, China*
[3]*Department of Orthopaedics and Traumatology, Nanfang Hospital, Southern Medical University, Guangzhou 510515, China*

Correspondence should be addressed to Bin Chen; chb@smu.edu.cn and Du Cheng; chengdu@mail.sysu.edu.cn

Received 27 January 2020; Revised 14 March 2020; Accepted 23 March 2020; Published 4 May 2020

Guest Editor: Liyuan Zhang

The dual-modified dendrimer containing dexamethasone (DET) and phenylalanine (Phe) was prepared to deliver plasmid DNA encoding dCas9 and single-guide RNA (sgRNA) for specific upregulation of β-defensin. DET and Phe moieties synergistically enhanced the transfection efficiency and reduced cytotoxicity of dendrimers. Combination of three sgRNAs targeting β-defensin gene demonstrated higher activation efficacy of β-defensin than any single sgRNA and combinations of any two sgRNAs, showing an efficient inhibition of virus infection and replication. The titer of vesicular stomatitis virus (VSV) in the cells treated with dCas9-sgRNA targeting β-defensin was reduced by about 100-fold compared to that of cells treated with dCas9-scramble sgRNA (dCas9-scr sgRNA). *In vivo* experiments demonstrated that the DET- and Phe-modified dendrimer effectively delivered plasmid DNA encoding dCas9 protein into the airway epithelium, inducing β-defensin expression. Delivery of the CRISPR activation system by a dendrimer modified with DET and Phe was a promising approach against viral disease.

1. Introduction

Identification of small molecules and vaccines for antiviral therapy is time consuming and laborious. In particular, little knowledge about emerging viruses makes it difficult to develop specific drugs or vaccines in a short time. Therefore, an alternative approach is needed against viral diseases. Except for targeting viral genome and protein, targeting host factors (i.e., innate system, adaptive immune apparatus, and other host genes) is an effective strategy to prohibit virus infection or replication. For example, maraviroc prevents cell entry of HIV and HBV virus by blocking human cellular protein CCR [1, 2]. However, only a few small molecules targeting host cellular proteins have been screened to treat viral diseases. Recently, emerging genetic manipulation technologies, including zinc-finger nucleases (ZNF), transcription activator-like effector nucleases (TALEN), and clustered regularly interspaced short palindromic repeats/Cas9 (CRISPR/Cas9) system, have provided powerful tools for inhibiting or activating host gene expression [3–5].

Among these technologies, the CRISPR/Cas9 system, a complex of Cas9 protein with single-guide RNA (sgRNA, a combination of the transactivating CRISPR RNA and spacer transcript CRISPR RNA), has attracted considerable attention because of its multiple gene regulation manners. sgRNA directs Cas9 protein to cleave its complementary double-stranded DNA. Upon cleavage by Cas9 protein, the target site is repaired *via* nonhomologous end joining (NHEJ) or homology-directed repair (HDR) mechanisms. Moreover, CRISPR activation (CRISPRa) and interference (CRISPRi) systems based on inactive Cas9 (dCas9), which specifically bind to DNA sequence without cleavage activity, were exploited to repress and induce interested gene expression [6, 7]. As for CRISPRa, transcription activator VP16 or activation domain p65 was combined with dCas9 to transactivate multiple gene transcriptions. For instance, the

CRISPRa/dCas9 approach was used to activate endogenous APOBEC3G and APOBEC3B to prevent HIV infection [8].

Defensin is one kind of key factors of the innate immunity system, being first in line against microorganism pathogens [9, 10]. The predominant expression of β-defensins was detected in the barrier epithelial cells and was considered an ideal antiviral agent. However, high cost and easy degradation of human β-defensin limit its clinical use. Fortunately, the CRISPRa system provides an alternative approach against virus by upregulating β-defensin and thereby activating innate immunity.

Plasmid DNA encoding dCas9 protein and sgRNA is unable to enter into cells by themselves. Therefore, utilization of DNA delivery vectors is of great necessity. Viral vectors (e.g., adenovirus, adeno-associated virus (AAV), and lentiviral viruses) showed high delivery efficiency, but their limited DNA packaging capacity and potential chromosome integration remain to be major hurdles [11, 12]. In contrast, nonviral vectors are readily available, cost effective, and can efficiently incorporate siRNAs or Cas9-sgRNA plasmids into one nanosystem [13, 14]. Moreover, some vectors such as dendrimers were easily modified with moieties including hydrophobic groups and nuclear localization signal molecules, which significantly enhanced transfection efficiency [15, 16]. Hydrophobic phenylalanine conjugated on the surface of dendrimer enhanced cell uptake [17]. Dexamethasone can bind to the nucleic membrane and thereby facilitate DNA transport into the nucleus [18]. Cationic polymers modified with DET remarkably increased gene expression levels [19]. However, dual-modification with Phe and DET is rarely used to enhance transfection efficiency. Moreover, there are few issues about the antivirus strategy by enhancing the β-defensin expression using nonviral delivery of the CRISPRa system.

Herein, we developed a DET and Phe dual-modified cationic dendrimer G4 (Phe)-DET for the delivery of CRISPRa plasmids targeting β-defensin. *In vitro* and *in vivo* experiments were performed to confirm antiviral effects of G4 (Phe)-DET dendrimer-based nonviral CRISPRa.

2. Materials and Method

2.1. Materials. PAMAM dendrimer G4, phenylalanine, and trifluoroacetic acid (TFA) were obtained from Sigma Aldrich (St. Louis, USA). 1-Hydroxybenzotriazole (HOBT), O-benzotriazole-N,N,N′,N′-tetramethyl-uronium-hexafluorophosphate (HBTU), dexamethasone, methanesulfonyl chloride, and 2-iminothiolane·HCl (Traut's reagent) were purchased from J&K Scientific (Beijing, China). The cells including human lung adenocarcinoma A549, human kidney 293T, human bronchial epithelial cell 16HBE cell, and mouse neuroblastoma N_2a cell were purchased from ATCC. Vesicular stomatitis virus (VSV) was from ATCC (stain; Indiana, USA). Dulbecco's modified eagle medium (DMEM), penicillin-streptomycin, fetal bovine serum (FBS), and Dulbecco's phosphate-buffered saline (PBS) were purchased from Gibco BRL (Carlsbad, USA). Biological reagents were purchased from Life Technologies. Plasmid pSP-dCas9-VPR was a gift from Prof. George Church (Addgene plasmid # 63798) and the activator was VPR, a tripartite activator composed of activation domains of VP64, p65, and Rta. Plasmid pphU6-gRNA was obtained from Prof. Charles Gersbach (Addgene plasmid # 53188). sgRNAs were prepared using T7 High Yield RNA Synthesis Kit (New England Biolabs, NEB). Primers and sgRNA sequences are shown in Table S1.

2.2. Synthesis of Dendrimer. The phenylalanine-modified generation 4.0 (G4) PAMAM dendrimer was synthesized mainly by amidation between the carboxyl group of phenylalanine and the surface amino groups of G4 PAMAM dendrimer. Briefly, G4 PAMAM dendrimer (0.5 g, 0.035 mmol) was dissolved in anhydrous DMF (5 mL) under nitrogen gas protection. Boc-phenylalanines were added at different molar ratios (carboxyl group of phenylalanine: surface amino groups of G4 PAMAM dendrimer) of 25% and 50%, followed by the addition of 1-hydroxybenzotriazole (HOBT) and O-benzotriazole-N,N,N′,N′-tetramethyl-uronium-hexafluorophosphate (HBTU) at 1.25 molar equivalents of carboxyl in Boc-phenylalanine, serving as the condensation reagent and catalyst to the reaction. After stirring at room temperature for 2 d, the reaction solution was precipitated three times in the diethyl-ether to obtain yellow solid precipitate noted as G4 (Phe-Boc). To deprotect the tert-butoxycarbonyl (Boc) groups, the G4 (Phe-Boc) dendrimer dissolved in dichloromethane was added to 5 mL trifluoroacetic acid (TFA) for 6 h with continuous magnetic stirring. After removal of TFA by rotary evaporation, the resulting crude products were again dissolved in DMF and purified by three rounds of precipitation in acetone. Finally, the yellow product G4 (Phe) was obtained by vacuum drying.

DET, a glucocorticoid, was used to modify the PAMAM dendrimer. First, the mesylate-activated DET was prepared by substituting the terminal hydroxyl group of DET for mesylate. Under nitrogen protection, DET (0.11 g, 0.269 mmol) dissolved in anhydrous pyridine (5 mL) was added to methanesulfonyl chloride at 2 molar equivalent and then incubated in an ice bath for 12 h with stirring, followed by the addition of ice deionized water to precipitate crude products. The mesylate-activated DET was purified by recrystallization from ethanol-acetic ether. Next, Traut's reagent and dexamethasone mesylate in 2.5 mL anhydrous DMSO at 0.015 mmol (8 equiv. to G4 (Phe-Boc)) were slowly added to G4 (Phe-Boc) in 2.0 mL anhydrous DMSO under nitrogen protection. The mixture was stirred for 12 h at room temperature. Excessive amounts of cold ethyl acetate were used to precipitate the reaction products. The mentioned product was dissolved in 5 mL TFA and stirred for 6 h, followed by precipitation in ethyl ether. This precipitating procedure was repeated three times to obtain pale yellow G4 (Phe)-DET. The yield of G4 (Phe)-DET was 105 mg.

2.3. Preparation of Polyplexes. To prepare polyplexes for plasmid delivery, the plasmid solution (1 μg/μL) was added to the G4 (Phe) or G4 (Phe)-DET solution at various N/P ratios. The mixture solution was pipetted approximately 50 times and then allowed to stand for 35 min.

2.4. Characterization. ^{1}H-NMR spectra were recorded on a Varian 400 MHz spectrometer using D_2O and DMSO d_6 as the solvent at room temperature. To determine macromolecular weight distributions of the polymers, gel permeation chromatography (GPC) was performed, using an acetic acid buffer system (pH 5.0) as the mobile phase at a flow rate of 1.0 mL/min. The GPC system was equipped with a Waters 515 pump, an ultrahydrogel™ 500 column, an ultrahydrogel™ 250 column, and a Waters 2410 differential refractive index detector. Samples flowed through ultrahydrogel ™ 500 column and ultrahydrogel ™ 250 column in sequence. Size of polyplexes was determined with the utilization of dynamic light scattering (DLS). The polyplex solutions were filtered through a 450 nm filter. Measurements were performed at 25°C on 90 Plus/BI-MAS equipment (Malvern Panalytical, Malvern, United Kingdom). Data were collected on an autocorrelator with a 90° detection angle of scattered light. The measurement results were recorded as the mean ± standard deviation (SD) of three independent measurements. Transmission electron microscopy (TEM) observations of the polyplexes were conducted using a Philips CM120 transmission electron microscope (Philips, Eindhoven, the Netherlands) at an accelerating voltage of 80 kV. Samples were prepared by drying a drop (10 μL) of the sample solution on a copper grid coated with amorphous carbon. For the sample staining, a small drop of uranyl acetate solution (1.5 wt% in water) was dropped on the copper grid and after 1 min blotted off with filter paper. Finally, the grid was dried overnight in a desiccator prior to TEM observation.

2.5. Gel Retardation Assay. To assess the plasmid DNA-binding ability of G4 $(Phe)_{25\%}$, G4 $(Phe)_{50\%}$, and G4 $(Phe)_{50\%}$-DET, gel electrophoresis was performed (Bio-Rad Laboratories, Inc., USA). Dendrimers were first dissolved in PBS (pH 7.4). Then, plasmids were added to the dendrimer solution to prepare polyplexes on preset N/P ratios, followed by standing for 35 min at room temperature. The polyplexes were loaded into 1% agarose gels with GoldenView (Beijing BLKW Biotechnology Co., Ltd., China). The retardation of plasmid DNA mobility was detected with UV light and imaged on DNR Bio-Imaging Systems (DNR Bio-Imaging System Ltd., Israel).

2.6. Cell Viability Assay. A549, 293T, and N_2a cells were cultured in DMEM containing 10% fetal bovine serum (FBS) in a humidified atmosphere of 5% CO_2 at 37°C. The cells were seeded into 96-well plates at a density of 1×10^3 cells/well. After incubating overnight at 37°C, cells were further incubated with Lipofectamine 2000, G4 $(Phe)_{25\%}$, G4 $(Phe)_{50\%}$, and G4 $(Phe)_{50\%}$-DET, which were combined with plasmid-GFP at various concentrations for 48 h, and cell viability was measured using MTT assay. Briefly, cell culture medium was replaced with 100 μL fresh DMEM containing 10 μL MTT solution (5 mg/mL in PBS) and then incubated for an additional 3 h at 37°C. After discarding the medium, 100 μL DMSO was added to dissolve the generated substrate for 15 min. The absorbance at 570 nm was measured using a Tecan Infinite F200 (Crailsheim, Germany). All experiments were conducted in triplicate.

2.7. Confocal Laser Scanning Microscopy (CLSM). A549, 293T, and N_2a cells were seeded in 35 mm glass-bottom dishes in 2 mL of DMEM containing 10% FBS at a density of 1×10^3 per plate. After incubation for 24 h, the medium was replaced with fresh opti-MEM containing polyplexes. The nuclei were stained with Hoechst 33342 (Beyotime Biotech, China) for 15 min. The cells were incubated at 37°C and imaged at designated times using a Zeiss LSM 710 confocal laser scanning microscope (Carl Zeiss, Oberkochen, Germany). GFP and Hoechst 33342 were excited at 488 and 352 nm and detected at 515 and 460 nm, respectively.

2.8. Quantity of Gene Expression. The expression of β-defensin in the transfected A549, 293T, and N_2a cells was evaluated at the mRNA level. Total RNA was extracted from cells using the RNeasy Micro Kit (Qiagen Inc., USA). The first-strand cDNA was synthesized using RNase H reverse transcriptase and random primers according to the manufacturer's protocol (Invitrogen, USA). cDNA (1 μg) was synthesized from the total RNA using PrimeScript™ RT reagent Kit (Takara, Japan). The mRNA expression of β-defensin was quantified with real-time PCR System using a FastStart Universal SYBR Green Master (ROX) Kit (Roche, Switzerland). The mRNA level of β-actin was also measured as an internal normalization standard. The primer and probe sequences are listed in Table S1. The real-time PCR program was run on a StepOnePlus Real-time PCR System (ABI, USA) at the thermal cycling conditions of 95°C for 10 min, followed by 40 cycles of 95°C for 30s, 58°C for 15 s, and 68°C for 15 s.

2.9. In Vitro Prevention of VSV Infection. A549 cells were seeded in 12-well plates at a density of 3×10^5 cells per well and incubated in DMEM at 37°C under a humidified atmosphere of 5% CO_2. After incubation overnight, the medium was replaced with fresh medium containing polyplexes. The amount of G4 $(Phe)_{50\%}$-DET was complexed with plasmids encoding dCas9 and sgRNA (1 μg) at N/P of 8. After incubation with polyplexes for 24 h, VSV was added to the medium at a titer of 100. The status of virus infection was detected by flow cytometry and inverted fluorescence microscopy. The culture supernatant was serially diluted 10-fold with DMEM and inoculated into the cells in 6-well plates for virus plaque assay. After 3 d of cultivation, titration of VSV was determined. All measurements were conducted three times for statistical analysis.

After being washed thrice with PBS, cells were harvested by trypsinization, centrifuged at 1,500 rpm for 5 min, and resuspended in 500 μL PBS. A Gallios flow cytometer (Beckman Coulter, California, USA) was used to evaluate the quantitative transfection efficiency by using a 488 nm laser for excitation and emission fluorescence of Alexa Fluor® 515 collected through a TRITC filter. For the evaluation of the GFP gene expression after the incubation with polyplexes, the cells were harvested according to the abovementioned method and subjected to flow cytometry. Typically,

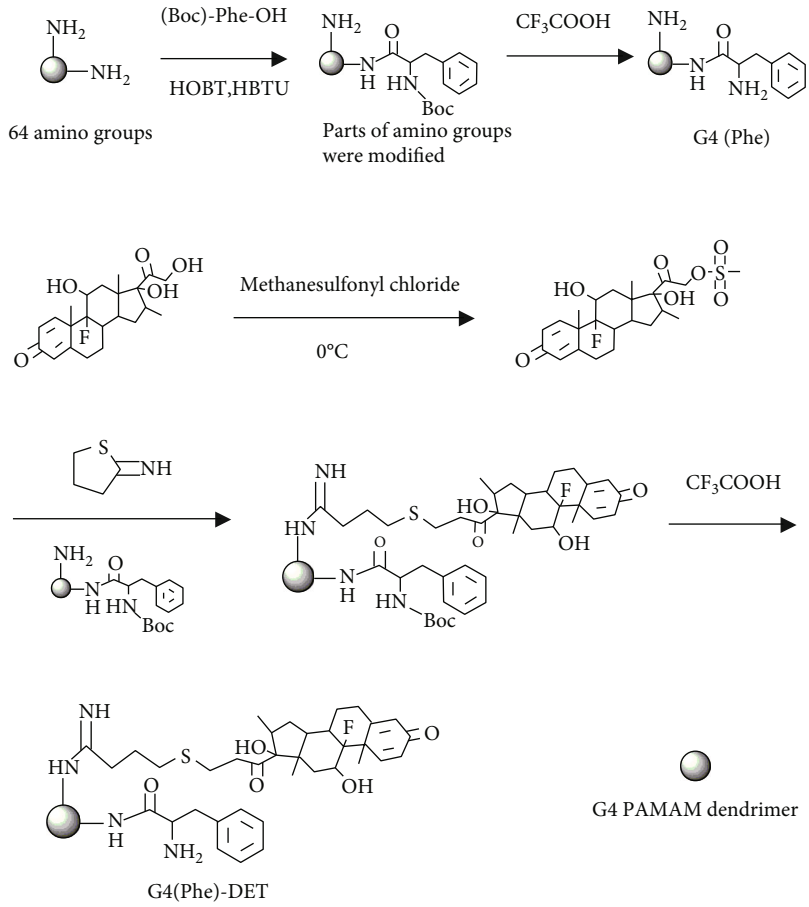

Figure 1: Synthetic route of G4 (Phe) and G4 (Phe)-DET.

cultured cells without transfection were used as controls for background calibration. Kaluza software (Version 1.2, Beckman Coulter, Inc. USA) was used to analyze the data.

2.10. In Vivo Studies. Female BALB/C mice (6–8 weeks old) were purchased from Guangdong Medical Laboratory Animal Center and kept in SPF animal center of School of Life Sciences, Sun Yat-sen University. All surgical interventions and postoperative animal care were conducted in accordance with the guidelines of the Council for the Purpose of Control and Supervision of Experiments on Animals, the Ministry of Health, and the government of China. After anesthetization via the tail vein by pentobarbital sodium at a dose of 50 mg/kg, the mice were administered polyplexes through the bronchus. The lungs were excised and subjected to detect the expression of the defensin gene. For the molecular biology assays, lung tissues were homogenized after being frozen in liquid nitrogen. Total RNA was extracted and analyzed as described in Section 2.8.

2.11. Histology and Immunohistochemistry. Mice were sacrificed, and their lungs were fixed in 4% paraformaldehyde for at least 24 h to obtain paraffin sections (2 μm) or frozen sections (5 μm). The paraffin sections were stained with H&E, and the images of the lung were assessed for the toxic effect in different treatment groups. The immunofluorescence staining for frozen sections was described briefly as follow: after blocking with 5% BSA for 0.5 h at 37°C, the frozen tissue sections were incubated with rabbit polyclonal primary antibodies for β-defensin (1 : 100 dilution in PBS/Tween; Cell Signaling Technology, Danvers, USA) and mouse monoclonal antibodies for Cas9 (Abcam, UK) overnight at 4°C. Then, AF647-labeled secondary antibody and AF488-labeled secondary antibody (Abcam, UK) were used to mark the β-defensin and dCas9 protein, respectively. After labeling the nuclei with DAPI, the tissue sections were scanned under CLSM.

2.12. Statistics. All experiments were carried out at least in triplicates. All data was indicated as mean ± standard deviation (SD). The statistical significance was determined by two-sided Student's t-test using Prism 5.0 ($^{*}p < 0.05$, $^{**}p < 0.01$, and $^{***}p < 0.001$).

3. Results

3.1. Preparation and Characterization of Dendrimer and Polyplex. DET- and Phe-modified dendrimers were prepared (Figure 1). First, Boc-protected Phe moieties were conjugated to dendrimer G4 *via* amidation between carboxyl groups of

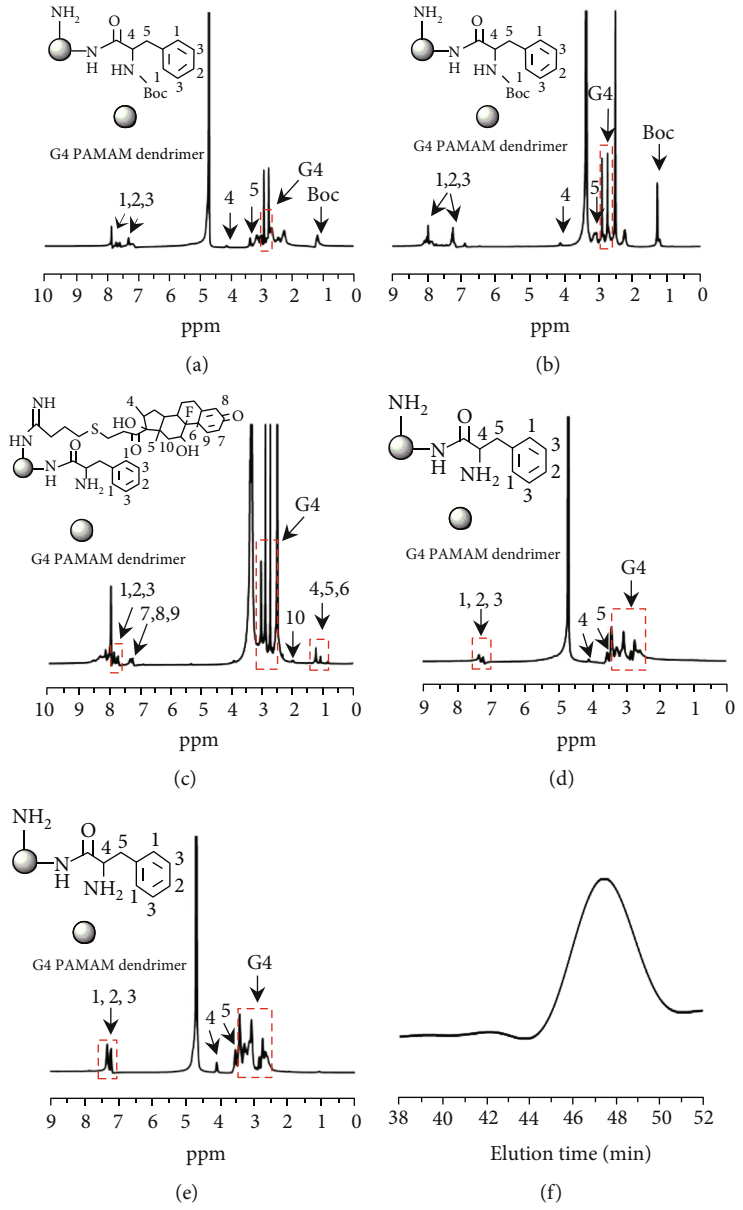

FIGURE 2: (a) ^{1}H-NMR spectra of G4 (Phe-Boc)$_{25\%}$, (b) G4 (Phe-Boc)$_{50\%}$, (c) G4 (Phe)$_{50\%}$-DET, (d) G4 (Phe)$_{25\%}$, and (e) G4 (Phe)$_{50\%}$. (f) GPC spectrum of G4 (Phe)$_{50\%}$-DET.

Boc-phenylalanine and facial amino groups of dendrimer at the molar ratios of 0.25 and 0.5, followed by deprotection of the Boc groups. The products were denoted as G4 (Phe)$_{25\%}$ and G4 (Phe)$_{50\%}$. Dexamethasone mesylate (DET-Mes) was introduced onto the surface of G4 (Phe-Boc) in the presence of Traut's reagent (2-iminothiolane hydrochloride). Finally, dendrimer G4 (Phe)-DET was obtained after removing the Boc groups, which was confirmed by the disappearance of the characteristic peak attributing to Boc at 1.2-1.4 ppm in the ^{1}H-NMR spectrum (Figure 2). DET-Mes was synthesized by conjugating a sulfonyl group with DET. The mentioned products were characterized by ^{1}H-NMR and GPC. The characteristic resonance peaks of the G4 dendrimer scaffold (C**H**$_2$ at 2.65-3.10 ppm) and phenylalanine (C**H** at 4.05-4.20 ppm, C**H**$_2$ at 3.5-3.75 ppm, and C**H** on the benzene ring of phenylalanine at 7.20-7.90 ppm) were observed, indicating successful synthesis of dendrimer G4 (Phe). Appearance of characteristic resonance peaks (0.9-1.3 ppm, CH$_3$, and 7.0-7.3 ppm, C**H** in dexamethasone) demonstrated that DET was conjugated with G4 (Phe). Composition of products was calculated according to the integration value of characteristic peaks attributing to G4 and Phe at 7.20-7.90 ppm, respectively. Conversion of the amino group in G4 (Phe)$_{25\%}$ and G4 (Phe)$_{50\%}$ was 22% and 47%, respectively. In the GPC chromatogram, G4 (Phe)$_{50\%}$ modified with DET (named as G4 (Phe)$_{50\%}$-DET) showed a unimodal molecular weight distribution (Figure 2(f)).

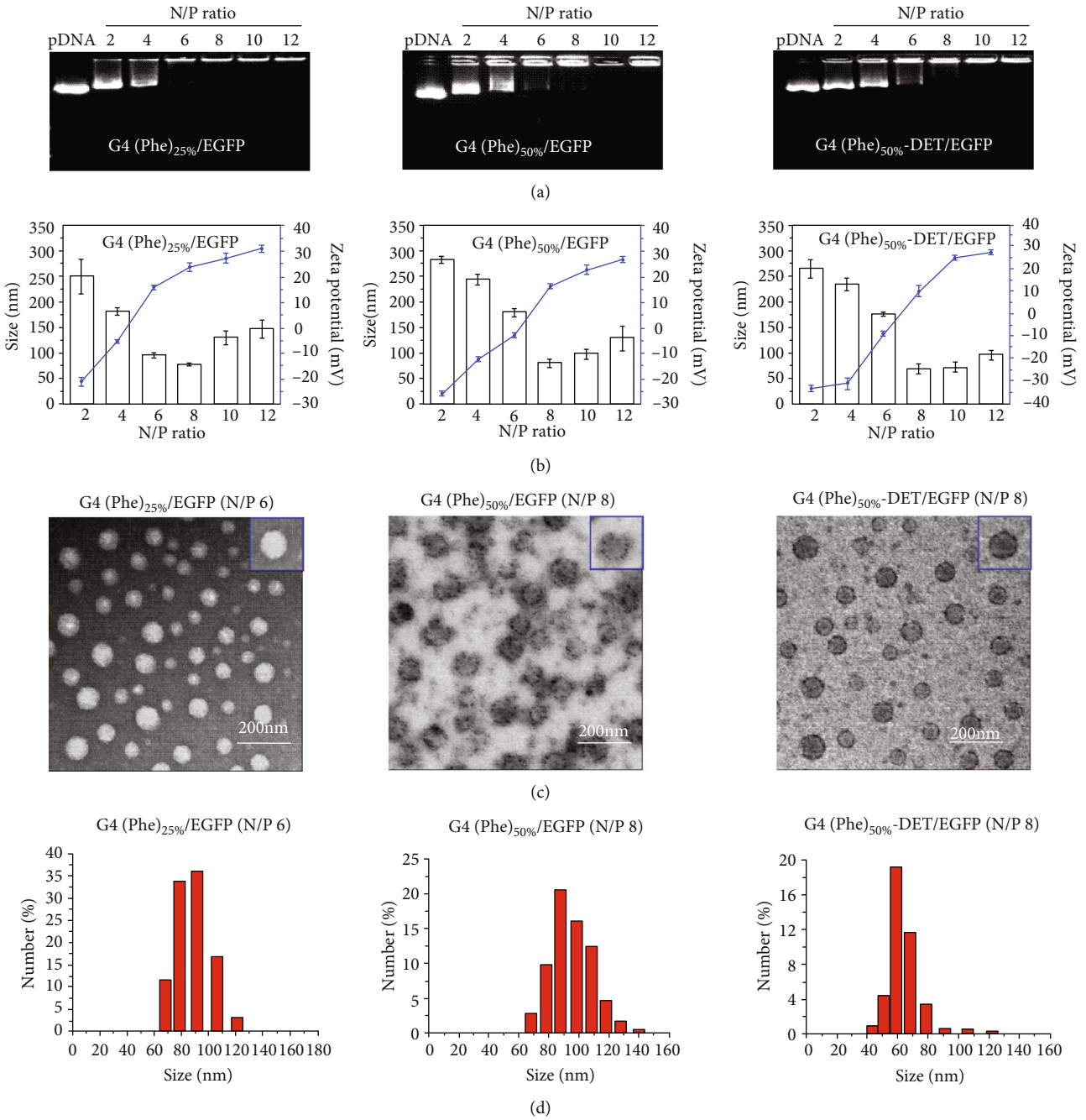

FIGURE 3: (a) Electrophoretic mobility of EGFP plasmid in agarose gel after complexing with G4 $(Phe)_{25\%}$, G4 $(Phe)_{50\%}$, and G4 $(Phe)_{50\%}$-DET at various N/P ratios. (b) Sizes and zeta potentials of G4 $(Phe)_{25\%}$/EGFP, G4 $(Phe)_{50\%}$/EGFP, and G4 $(Phe)_{50\%}$-DET/EGFP complexes at different N/P ratios. (c) Transmission electron microscopy (TEM) images and (d) DLS of G4 $(Phe)_{25\%}$/EGFP at N/P of 6, G4 $(Phe)_{50\%}$/EGFP at N/P of 8, and G4 $(Phe)_{50\%}$-DET/EGFP at N/P of 8. Results are presented as the mean ± SD ($n = 3$).

Complexation of plasmids with various dendrimers was evaluated by gel retardation assay. Disappearance of the DNA band in agarose indicates full neutralization of the negative charge of plasmid [20, 21]. As shown in Figure 3, G4 $(Phe)_{25\%}$ completely retarded DNA migration above N/P ratio of 6, but the dendrimer G4 $(Phe)_{50\%}$ achieved complete retardation above N/P ratio of 8, indicating that Phe modification reduced the DNA complexation ability of the dendrimer due to the charge shielding effect of the Phe hydrophobic benzene ring and the low surface charge density [17, 22]. The modification of DET has no significant impact on the DNA complexation ability of dendrimer G4 $(Phe)_{50\%}$-DET. Furthermore, sizes and zeta potentials of polyplexes under various N/P ratios were investigated by dynamic light scattering (DLS). As shown in Figure 3(b), zeta potentials of all dendrimers/EGFP complexes were converted to positive

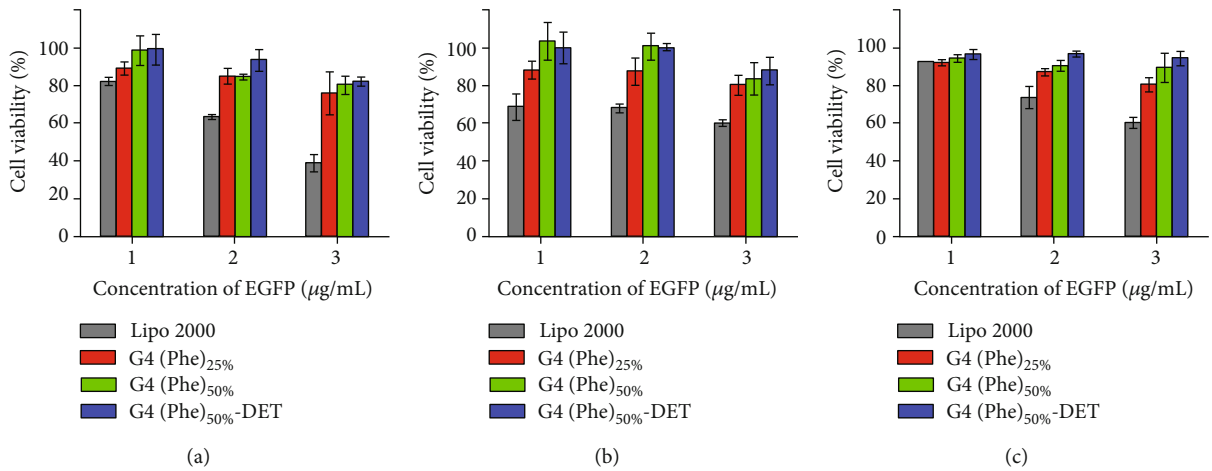

Figure 4: Cell viability of dendrimers to (a) human kidney 293T cells, (b) mouse neuroblastoma N_2a cells, (c) and human lung adenocarcinoma A549 cells. Incubation time: 48 h. Dose: 55.6 μM. Complexes were prepared at N/P of 6 for G4 $(Phe)_{25\%}$/EGFP, N/P of 8 for G4 $(Phe)_{50\%}$/EGFP, and N/P of 8 for G4 $(Phe)_{50\%}$-DET/EGFP, respectively. The concentrations of EGFP plasmid were 1, 2, and 3 μg/mL, respectively.

from negative when N/P ratio was above 6, and sizes were kept constant. At N/P ratio of 8, the zeta potentials of G4 $(Phe)_{25\%}$/EGFP complexes, G4 $(Phe)_{50\%}$/EGFP complexes, and G4 $(Phe)_{50\%}$-DET/EGFP complexes were around +23, +16, and +10 mV, respectively. At N/P ratio of 8, G4 $(Phe)_{50\%}$-DET/EGFP complexes had a smaller size than other complexes. With the excessive input of polymer (at higher N/P ratios), complexes held more positive charge and swelled maybe due to the electrostatic repelling effect between the positively charged chains. Consequently, size of G4 $(Phe)_{50\%}$-DET/EGFP complexes increased to 93.9 nm at N/P of 12. The sizes and zeta potentials of G4 $(Phe)_{50\%}$/EGFP and G4 $(Phe)_{25\%}$/EGFP complexes showed similar trends. TEM images showed that three complexes were sphere with a uniform size around 70-80 nm (Figure 3(c)), which was in line with that determined by dynamic light scattering (DLS) (Figure 3(d)).

3.2. Cytotoxicity and Cell Uptake. Although high positive surface charge is favorable for cell uptake of polyplexes, it also leads to apparent cytotoxicity to cells. Hence, it is necessary to balance these two factors. Introducing a hydrophobic moiety such as phenylalanine on the surface of dendrimer can effectively reduce its cytotoxicity and increase its affinity to cells [17]. As expected, Phe modification significantly decreased the cytotoxicity of G4 dendrimers to 293T, N_2a, and A549 cells (Figure 4). The dendrimer modified with Phe and DET slightly increased cell viability when compared with Phe-modified dendrimers. Notably, the single and dual modification with Phe and DET both enhanced transfection efficiency at various levels. In this study, the transfection efficiency of various dendrimers was evaluated in 293T, N_2a, and A549 cells using EGFP- (enhanced green fluorescence protein-) encoding plasmid as a reporter (Figure 5). The enhancement of transfection efficiency was attributed to two reasons: (1) the interaction between hydrophobic phenylalanine and the hydrophobic region of the cell membrane resulted in the destabilization of the cell membrane, thereby promoting translocation of the plasmid across the cell membrane and (2) DET guided plasmid into the nucleus [18]. The highest transfection efficiency was recorded in the cells receiving dendrimer modified with both Phe and DET, indicating that the dual modification synergistically enhanced transfection efficiency.

3.3. Antivirus Effect of CRIPSR/dCas9 by Upregulating β-Defensin. Several plasmids carrying sequences encoding sgRNA targeting the β-defensin promoter region were designed and delivered to human cells (A549, 293T, and 16HBE) and mouse cells (N_2a). The mRNA level of β-defensin was evaluated through real-time quantitative PCR, and the results are shown in Figure 6 and S1. For A549 human cells, treatment with sg5, sg7, and sg9 sgRNA complexed with G4 $(Phe)_{50\%}$-DET upregulated β-defensin by 10, 15, and 40 times in comparison with scramble sgRNA plasmid (scr sgRNA plasmid) treatment, respectively. Importantly, combination of three sgRNA plasmids (sg5+sg7+sg9) had higher mRNA copies of β-defensin than other treatments. The sgRNA (sg5+sg7+sg9) treatment enhanced gene expression by 10, 3, and 1.5 times compared with two sgRNA treatments (sg5+sg7, sg5+sg9, and sg7+sg9). Moreover, in 293T cells, the identified sgRNA treatments presented a much greater enhancing effect by around 45000 times compared to the scr sgRNA treatment (Figure 6(b)). Similar results were also confirmed in mouse N_2a cells. As shown in Figure 6(c) and S1, combination of sg2 and sg3 sgRNA (sgMBD4) increased β-defensin gene expression by about 25 times.

The antiviral effect of nonviral CRISPR/dCas9 targeting β-defensin was evaluated by plaque formation and flow cytometry assays. To monitor virus infection, A549 cells were coincubated with vesicular stomatitis virus incorporating the

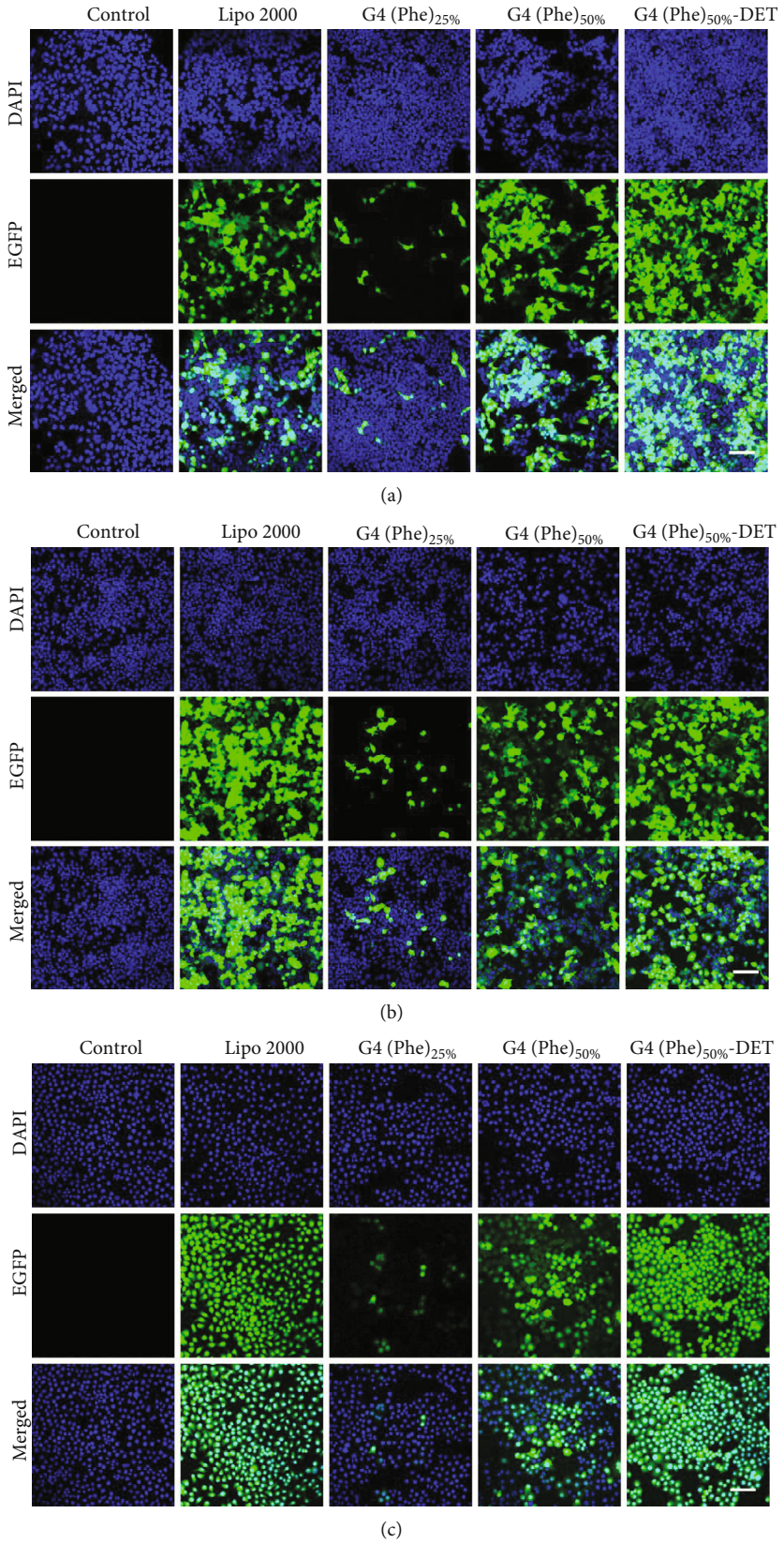

Figure 5: Confocal laser scanning microscopy (CLSM) images of human kidney 293T cells (a), mouse neuroblastoma N_2a cells (b), and human lung adenocarcinoma A549 cells (c) incubated with Lipo2000/plasmid, G4 $(Phe)_{25\%}$/plasmid, G4 $(Phe)_{50\%}$/plasmid, and G4 $(Phe)_{50\%}$-DET/plasmid. Incubation time: 48 h. Nuclei: stained blue with DAPI; green fluorescence: EGFP protein. Scale bars represent 100 μm.

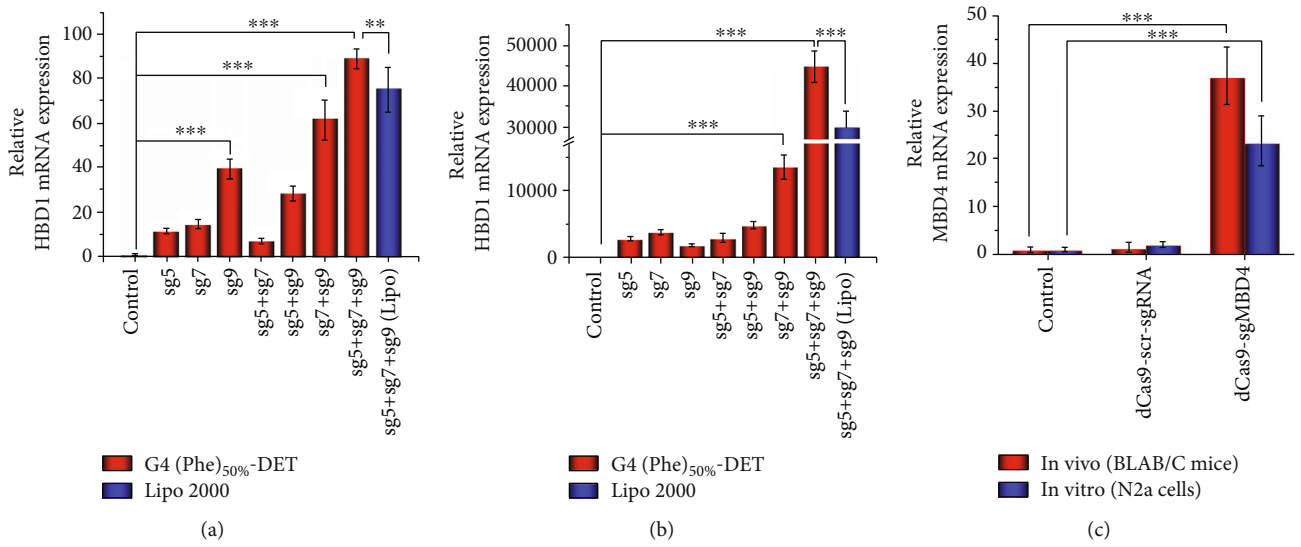

FIGURE 6: *In vitro* and *in vivo* relative β-defensin mRNA expression quantified by real-time PCR analysis in the human lung adenocarcinoma A549 cells (a), human kidney 293T (b), mouse neuroblastoma (*in vitro*), and BLAB/C mice (*in vivo*) (c). Dose: 1 μg/μL dCas9 plasmid and 1 μg/μL sgRNA plasmid were complexed with G4 $(Phe)_{50\%}$-DET/plasmid at N/P of 8 and Lipo2000 at N/P of 2. Inhalation dose: 5 μg/μL dCas9 plasmid and 5 μg/μL scr sgRNA or 5 μg/μL sgMBD4 in 100 μL PBS. Mouse neuroblastoma N_2a cells were used in *in vitro* experiments. BLAB/C mouse administrated with complexes was tested. MBD4 and HBD1 are abbreviations of mouse beta-defensin-4 and human beta-defensin-1, respectively. The scr sgRNA represented nonsense sgRNA and sgMBD4 represented mouse β-defensin-4 sgRNA (sg2+sg3) with the highest expression at mRNA level. Data are mean ± SD ($n = 3$). $^{**}p < 0.01$, $^{***}p < 0.001$.

GFP gene as a reporter (VSV-GFP). As shown in Figure 7, treatments with dCas9 alone and dCas9-scr sgRNA showed GFP-positive cells of 86.1% and 78.6%, respectively, indicating that dCas9 without sgRNA targeting β-defensin cannot block virus invasion. However, dCas9-sgHBD1 treatment significantly reduced the percentage of GFP-positive cells from 86.1% to 42.9%. Results of virus titer were consistent with those of flow cytometry. The titer value of cells receiving dCas9-sgHBD1 treatment decreased by about 100 times compared to that of cells receiving empty vector and dCas9-scr sgRNA treatments (Figures 7(a) and 7(b)). These results demonstrated that the delivery of dCas9-sgHBD1 with Phe- and DET-modified dendrimers remarkably prevented virus infection and replication.

3.4. In Vivo Studies. First, *in vivo* upregulation of β-defensin was evaluated after delivery of the CRISPRa system using Phe and DET dual-modified dendrimers. The nanoparticles containing 5 μg/μL dCas9 plasmids and 5 μg/μL sgRNA plasmids were prepared at N/P of 8 and intratracheally administrated into the mouse respiratory tract according to the approach [23]. Two days after inhalation administration, the lung and respiratory tract were excised and subjected to molecular biological and histological analyses [24]. Treatment with dCas9-sgMBD4 induced β-defensin gene expression by about 40-fold compared with dCas9-scr sgRNA treatment (Figure 6). As shown in Figure 8, evident dCas9 and β-defensin proteins were observed in the lung tissue sliced from mice receiving treatment with dCas9-sgMBD4. No β-defensin proteins were observed in the lung tissue from mice receiving no sgRNA or scr sgRNA treatment. In addition, the nanoparticles showed no significantly detrimental effects on the lung tissue.

4. Discussion

PAMAM dendrimers with globular structures and positively charged surfaces have been widely used as gene transfection reagents because of their ability to condense DNA and interact with cell membranes [25]. However, membrane barriers including outer cell membrane and inner nuclear membrane limited gene delivery efficiency of dendrimer carriers. Thus, several approaches have been developed to overcome these barriers by conjugating dendrimers with hydrophobic moieties and substances related to nuclear localization [15–18]. First, the hydrophobic phenylalanine was modified on the shell of the dendrimers to improve transfection activity. Interaction between phenylalanine residues and hydrophobic regions in the cell membrane destabilized the membrane and enhanced translocation of polyplexes across the cell membrane. Besides, density of phenylalanine on the surface of the dendrimer also had an impact on transfection efficiency. The dendrimer modified with high density of hydrophobic phenylalanine (50%) showed higher transfection efficiency (Figure 5), which was in line with the result that the dendrimer with 50% substitution of phenylalanine exhibited better transfection activity than other substitutions of 10% and 20% [17]. Second, several nuclear localization signal peptides and small molecules (e.g., DET) were used to translocate polyplexes into the nucleus. For example, dexamethasone-modified dendrimers or DNA enhanced their accumulation in the nucleus due to the translocation and the dilation of

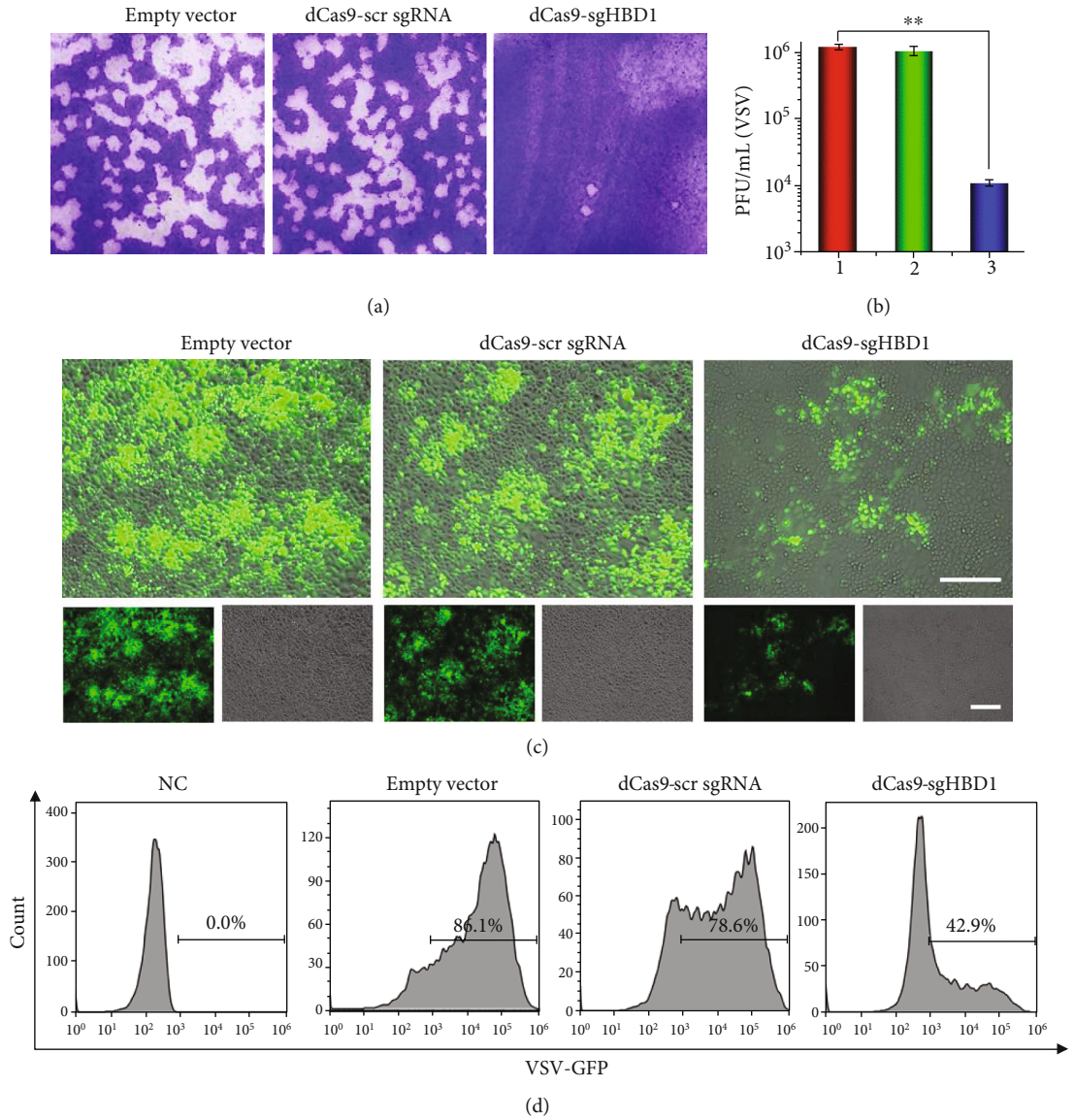

Figure 7: (a) Virus plaque images and (b) virus titer. Empty vector: G4 $(Phe)_{50\%}$-DET without plasmids; dCas9-scr sgRNA: G4 $(Phe)_{50\%}$-DET complexed with dCas9 and scr sgRNA plasmids; dCas9-sgHBD1: G4 $(Phe)_{50\%}$-DET complexed with dCas9 and HBD1 sgRNA plasmids; NC indicates mice receiving PBS treatment. Viral titers in cell culture medium were detected by plaque assay. Data were presented as mean ± SD of three independent experiments. $^{**}p < 0.01$. The "1," "2," and "3" of the X axis represent samples receiving empty vector, dCas9-scr sgRNA, and dCas9-sgHBD1 treatments, respectively. (c) Inverted fluorescence microscopy images of A549 cells receiving different treatments followed by VSV-GFP virus infection. Green fluorescence: VSV-GFP. Scale bars represent 250 μm. (d) Flow cytometry analysis of the green fluorescence- (GFP-) positive cells in samples receiving different treatments. Complexes were prepared for G4 $(Phe)_{50\%}$-DET/dCas9-sgRNA at N/P of 8. scr sgRNA represented nonsense sgRNA and sgHBD1 represented mixture of human β-defensin-1 sgRNA (sg5+sg7+sg9).

nuclear pores by the receptor of DET [18, 19]. Therefore, dual modification with Phe and DET may synergistically enhance transfection efficiency by overcoming plasma and nuclear membranes.

The limited resources of human β-defensin have hindered its clinical application. The CRISPRa technology provides a powerful and feasible approach to prohibit virus invasion by upregulating human β-defensin. The CRISPRa system was adopted to identify the host factor, beta-1,4-N-acetyl-galactosaminyltransferase 2 (B4GALNT2), which can abolish infection by inhibiting influenza virus binding to sialic acid receptors [26]. However, this strategy has rarely been explored to block virus infection *in vivo*. It is well known that a high level of β-defensin in the airway epithelium can effectively inhibit virus infection and replication [9, 10]. In this study, we utilized Phe and DET dual-modified dendrimer to deliver the CRISPRa system targeting the β-defensin gene, significantly reducing the VSV titer by

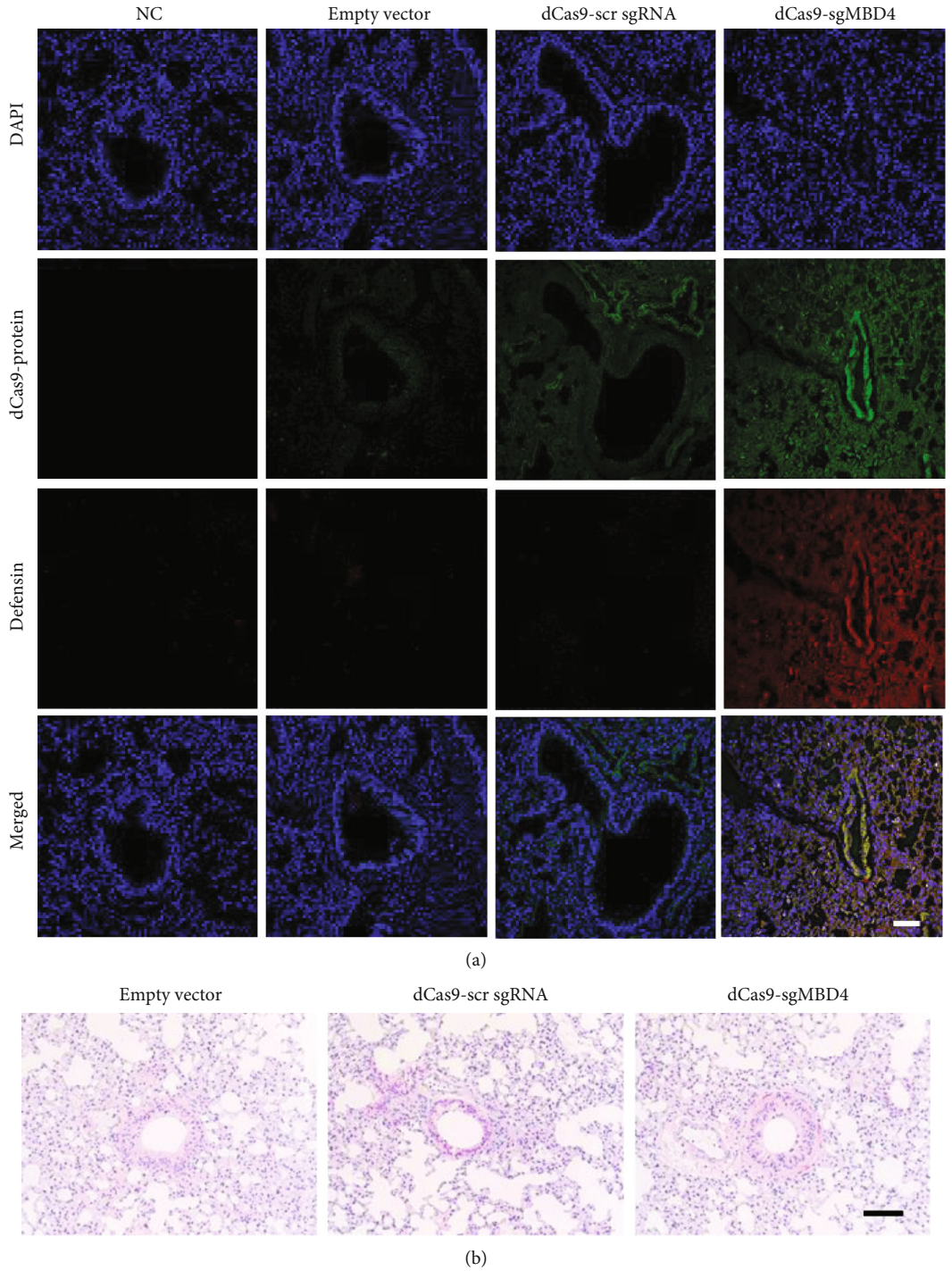

Figure 8: *Ex vivo* fluorescence immunohistochemical analyses (a) and histological characteristics (H&E stainning) (b) of lung sections from mice receiving different formulations (48 h after the inhalation). In the immunohistochemical assay, the nucleus, dCas9 protein, and β-defensin protein were stained blue, green, and red fluorescence, respectively. Inhalation dose: 5 μg/μL dCas9 plasmid and 5 μg/μL sgRNA (sgMBD4) in 100 μL PBS. Complexes were prepared at N/P value of 8. Scale bars, 100 μm in (a) and 50 μm in (b).

100-fold. CRISPR-Cas9/dCas9 causes off-target gene editing, but rationally engineered Cas9 or dCas9 can remarkably enhance specificity of gene editing [27]. Moreover, no gene disruption of dCas9-mediated CRISPRa also improved its biosafety. Except nuclear-localizing effect, dexamethasone can also improve therapeutic effects of the antivirus drug via reducing inflammation as a glucocorticoid.

5. Conclusion

The phenylalanine and dexamethasone dual-modified dendrimer was synthesized to transport the CRISPR/dCas9-sgRNA targeting β-defensin against virus infection. Phenylalanine and dexamethasone synergistically enhanced transfection efficiency, resulting in significantly antiviral activity.

Data Availability

The data used to support the findings of this study are included within the article

Conflicts of Interest

The authors declare that they have no conflicts of interest.

Authors' Contributions

Mingxiang Zuo and Xiaoxia Li contributed equally to this work.

Acknowledgments

This work was supported by the National Key R&D Program of China (2016YFE0117100), the National Natural Science Foundation of China (21875289 and U1501243), the Guangdong-Hong Kong Joint Innovation Project (2016A050503026), the Major Project on the Integration of Industry, Education and Research of Guangzhou City (201704030123), the Science and Technology Program of Guangzhou (201704020016), the Guangdong Innovative and Entrepreneurial Research Team Program (2013S086), and the Guangdong Province Science and Technology Innovation Special Fund (International Scientific Cooperation, 2018A050506035).

Supplementary Materials

The supplement file include Figure S1 and Table S1. Relative mRNA expression in cells receiving dCas9 and sgRNA plasmids delivered with Lipofectamine 2000 were reported in Figure S1; and Sequences of sgRNAs and primers were described in Table S1. *(Supplementary Materials)*

References

[1] J. Wheeler, M. McHale, V. Jackson, and M. Penny, "Assessing theoretical risk and benefit suggested by genetic association studies of CCR5: experience in a drug development programme for maraviroc," *Antiviral Therapy*, vol. 12, no. 2, pp. 233–245, 2007.

[2] L. Waters, A. Jackson, L. Else et al., "Switching safely: pharmacokinetics, efficacy and safety of switching efavirenz to maraviroc twice daily in patients on suppressive antiretroviral therapy," *Antiviral Therapy*, vol. 20, no. 2, pp. 157–163, 2015.

[3] J. C. Miller, S. Tan, G. Qiao et al., "A TALE nuclease architecture for efficient genome editing," *Nature Biotechnology*, vol. 29, no. 2, pp. 143–148, 2011.

[4] F. D. Urnov, E. J. Rebar, M. C. Holmes, H. S. Zhang, and P. D. Gregory, "Genome editing with engineered zinc finger nucleases," *Nature Reviews Genetics*, vol. 11, no. 9, pp. 636–646, 2010.

[5] W. Y. Hwang, Y. Fu, D. Reyon et al., "Efficient genome editing in zebrafish using a CRISPR-Cas system," *Nature Biotechnology*, vol. 31, no. 3, pp. 227–229, 2013.

[6] H. Zhou, J. Liu, C. Zhou et al., "*In vivo* simultaneous transcriptional activation of multiple genes in the brain using CRISPR-dCas9-activator transgenic mice," *Nature Neuroscience*, vol. 21, no. 3, pp. 440–446, 2018.

[7] M. H. Larson, L. A. Gilbert, X. Wang, W. A. Lim, J. S. Weissman, and L. S. Qi, "CRISPR interference (CRISPRi) for sequence-specific control of gene expression," *Nature Protocols*, vol. 8, no. 11, pp. 2180–2196, 2013.

[8] S. Chen, X. Yu, and D. Guo, "CRISPR-Cas targeting of host genes as an antiviral strategy," *Viruses*, vol. 10, no. 1, p. 40, 2018.

[9] W. Li, Y. Feng, Y. Kuang et al., "Construction of eukaryotic expression vector with mBD1-mBD3 fusion genes and exploring its activity against influenza a virus," *Viruses*, vol. 6, no. 3, pp. 1237–1252, 2014.

[10] T. Ganz, "Defensins: antimicrobial peptides of innate immunity," *Nature Reviews Immunology*, vol. 3, no. 9, pp. 710–720, 2003.

[11] F. A. Ran, L. Cong, W. X. Yan et al., "*In vivo* genome editing using Staphylococcus aureus Cas 9," *Nature*, vol. 520, no. 7546, pp. 186–191, 2015.

[12] H. Yin, K. J. Kauffman, and D. G. Anderson, "Delivery technologies for genome editing," *Nature Reviews Drug Discovery*, vol. 16, no. 6, pp. 387–399, 2017.

[13] G. Zhou, Y. Xu, M. Chen, D. Cheng, and X. Shuai, "Tumor-penetrating peptide modified and pH-sensitive polyplexes for tumor targeted siRNA delivery," *Polymer Chemistry*, vol. 7, no. 23, pp. 3857–3863, 2016.

[14] H. X. Wang, Z. Song, Y. H. Lao et al., "Nonviral gene editing via CRISPR/Cas 9 delivery by membrane-disruptive and endosomolytic helical polypeptide," *Proceedings of the National Academy of Sciences of the United States of America*, vol. 115, no. 19, pp. 4903–4908, 2018.

[15] C. Liu, T. Wan, H. Wang, S. Zhang, Y. Ping, and Y. Cheng, "A boronic acid-rich dendrimer with robust and unprecedented efficiency for cytosolic protein delivery and CRISPR-Cas 9 gene editing," *Science Advances*, vol. 5, no. 6, article eaaw8922, 2019.

[16] J. A. Kretzmann, D. Ho, C. W. Evans et al., "Synthetically controlling dendrimer flexibility improves delivery of large plasmid DNA," *Chemical Science*, vol. 8, no. 4, pp. 2923–2930, 2017.

[17] F. Wang, Y. Wang, H. Wang, N. Shao, Y. Chen, and Y. Cheng, "Synergistic effect of amino acids modified on dendrimer surface in gene delivery," *Biomaterials*, vol. 35, no. 33, pp. 9187–9198, 2014.

[18] Y. M. Bae, H. Choi, S. Lee et al., "Dexamethasone-conjugated low molecular weight polyethylenimine as a nucleus-targeting lipopolymer gene carrier," *Bioconjugate Chemistry*, vol. 18, no. 6, pp. 2029–2036, 2007.

[19] J. S. Choi, K. S. Ko, J. S. Park, Y. H. Kim, S. W. Kim, and M. Lee, "Dexamethasone conjugated poly (amidoamine) dendrimer as a gene carrier for efficient nuclear translocation," *International Journal of Pharmaceutics*, vol. 320, no. 1-2, pp. 171–178, 2006.

[20] J. Wu, J. Huang, S. Kuang et al., "Synergistic microRNA therapy in liver fibrotic rat using MRI-visible nanocarrier targeting hepatic stellate cells," *Advanced Science*, vol. 6, no. 5, article 1801809, 2019.

[21] J. Huang, C. Lin, J. Fang et al., "pH-sensitive nanocarrier-mediated codelivery of simvastatin and noggin siRNA for synergistic enhancement of osteogenesis," *ACS Applied Materials & Interfaces*, vol. 10, no. 34, pp. 28471–28482, 2018.

[22] K. Kono, H. Akiyama, T. Takahashi, T. Takagishi, and A. Harada, "Transfection activity of polyamidoamine dendrimers having hydrophobic amino acid residues in the periphery," *Bioconjugate Chemistry*, vol. 16, no. 1, pp. 208–214, 2005.

[23] B. J. Li, Q. Tang, D. Cheng et al., "Using siRNA in prophylactic and therapeutic regimens against SARS coronavirus in rhesus macaque," *Nature Medicine*, vol. 11, no. 9, pp. 944–951, 2005.

[24] B. J. Zheng, K. W. Chan, Y. P. Lin et al., "Delayed antiviral plus immunomodulator treatment still reduces mortality in mice infected by high inoculum of influenza A/H5N1 virus," *Proceedings of the National Academy of Sciences of the United States of America*, vol. 105, no. 23, pp. 8091–8096, 2008.

[25] S. D. Jativa, N. Thapar, D. Broyles et al., "Enhanced delivery of plasmid DNA to skeletal muscle cells using a DLC8-binding peptide and ASSLNIA-modified PAMAM dendrimer," *Molecular Pharmaceutics*, vol. 16, no. 6, pp. 2376–2384, 2019.

[26] B. E. Heaton, E. M. Kennedy, R. E. Dumm et al., "A CRISPR activation screen identifies a pan-avian influenza virus inhibitory host factor," *Cell Reports*, vol. 20, no. 7, pp. 1503–1512, 2017.

[27] I. M. Slaymaker, L. Gao, B. Zetsche, D. A. Scott, W. X. Yan, and F. Zhang, "Rationally engineered Cas9 nucleases with improved specificity," *Science*, vol. 351, no. 6268, pp. 84–88, 2015.